

Márk Venczel, György Bicsák, Árpád Veress

COUPLED FLUID DYNAMIC AND HEAT TRANSFER ANALYSIS OF A SMALL-SIZED RESEARCH GAS TURBINE COMBUSTION CHAMBER

In phase of design and development of gas turbine jet engines, it is indispensable to be aware of the complex physical, chemical, fluid dynamic, heat transfer and thermodynamic phenomena occurring inside the main engine parts. With use of CFD tools and visualisation techniques, engineers are able to reveal and better understand the elaborate and hidden processes in gas turbine engines. The aim of this study is to perform a coupled fluid dynamic and heat transfer analysis on a small-sized research gas turbine combustion chamber with special care for the accuracy of combustion process and outlet temperature distribution compared to the combustion-theory requirements and to available and suitable data for verification. The plausibility check was accomplished with the results of a MSc thesis and an ongoing PhD dissertation with same geometry and similar conditions and objectives.

Keywords: *CFD, combustion modelling, combustor, gas turbine jet engine, turbine inlet temperature*

1. INTRODUCTION

Nowadays, gas turbine jet engines are considered to be not only the relevant propulsion systems of the high power commercial and military aircrafts but the most practicable and economical machineries for energy production in gas and oil sectors. Their unprecedented advantages are the high power-weight index, few moving components, high reliability and availability, little sensitivity for overload and the fact that their operation does not require such type of liquid-based cooling system. Nevertheless, the maximum allowable temperature in the combustion chamber and at the turbine inlet section must be limited due to metallurgical reasons. To measure and monitor this temperature data in an operating combustor is always a difficult task due to the high temperature ranges and sudden heat loads, which do not allow the application of conventional thermometers. Additionally, the presence of measuring equipment can have a remarkable effect on the streamlines (wakes), pressure drop, heat transfer, mixing and combustion process which can lead to significant errors in the measured results. Thus the obvious solution is to use well validated CFD tools in order to perform virtual tests on a combustion chamber operation in more cost-, time- and capacity-efficient ways.

1.1 Gas turbine jet engine performance

Gas turbine jet engines involve three types of energy in a two-step energy transformation. The power of matter is stored in the fuel in form of chemical energy. A certain proportion of chemical energy is released during combustion as thermal energy and raises the power capacity of compressed air entering the combustion chamber. After this, during expansion the uniformly heated gas mixture with higher enthalpy (compared to ambient) leaves the combustor and drives the turbine. As a result, thermal energy is transferred into mechanical energy on the turbine blades and the engine generates shaft power or thrust.

As far as performance is concerned, the most important parameter of the engine, after the pressure ratio of the compressor, is the turbine inlet temperature (TIT). One way to enhance the thermal efficiency and specific power of the engine is to increase TIT. This can be realized by less intermediate, dilution and cooling air and/or increasing the pressure ratio which will result higher thermal load on the first set of rotor material blades and decreases the lifetime of turbine.

The very first gas turbines managed to reach the turbine inlet temperature value of only 400 °C but between the world wars, technology allowed to raise this number to 775 °C. In the late 1960s, aviation industry achieved a TIT of 1010 °C at the use of JT9D-7 gas turbine in the iconic Boeing 747-100. Nowadays, Rolls Royce Trent 1000 engine of Airbus 380 or the GE NX engine of Boeing 787 operate with 1500–1600 °C TIT. This performance could not be reached without a sophisticated cooling system as the result of thorough blade cooling and metallurgical developments with theoretical support of advanced material science (see **Figure 1**). On the one hand, high performance alloys (called superalloys) are used for turbine blades, which are capable of withstanding high temperature and stress in extremely oxidizing atmospheres and show favourable creeping properties with low cycle fatigue [1].

On the other hand, turbine blades can be cooled with fuel or with film cooling which provides thermal protection by forming a layer of cold air around the blades. In terms of combustor, the best way of cooling is called transpiration cooling, where the chamber wall is made of porous material that allows air to pass through it. Together with Thermal Barrier Coating system and air cooling passages the combustor and turbine blades are protected from prompt thermal fatigue. [2]

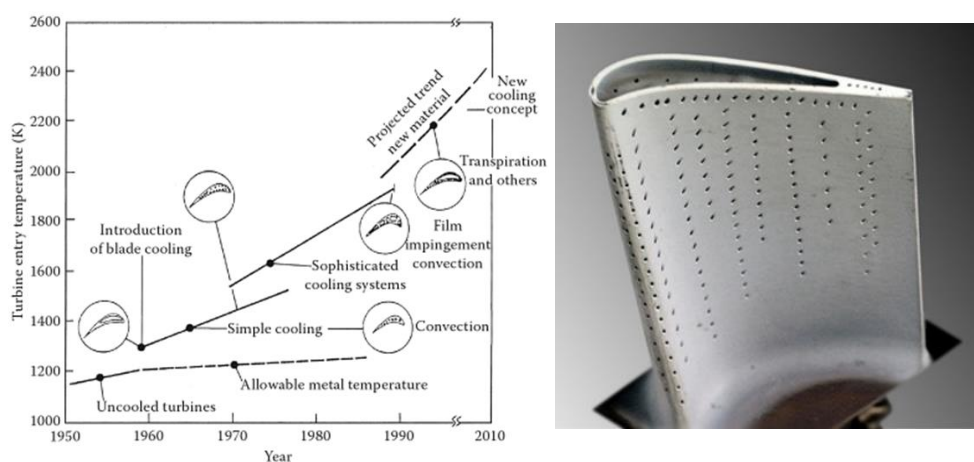


Figure 1 Development of turbine blade cooling (left) and film cooling holes on a turbine blade (right) [3][4]

It is clearly seen, that combustion is the key phenomenon which governs the engine performance. Because of its critical role, an accurate turbulent flame control is demanded so that we will be able to burn fuels more efficiently, raise performance by TIT and reduce pollutants in the exhausted gas. It appears as a real challenge to find accurate solution with help of CFD in the production of power.

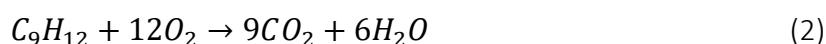
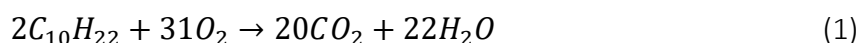
1.2 The combustion process

Combustion is believed the oldest and fundamental technology of humanity, which has been used for more than one million years in order to keep our world in development. It is a certain type of oxidation that can be described as a rapid chemical reaction between fuel (which con-

serves huge amount of energy stored in material) and oxidizer (which creates proper environment for burning). An activation energy is also needed for reactants to begin an exothermal process in form of self-propagating flames. In terms of gas turbine engines, combustion is a continuous phenomenon, where Jet-A (kerosene) plays the role of fuel while oxygen in the air is the oxidizer and activation energy is added as spark ignition.

Flame can be determined as the rapidly reacting body of hot gases, where the released chemical energy is emitted in the visible spectrum. The flame front or reacting zone is a small region where chemical reactions take place. Other physical phenomena can also accompany the combustion such as explosion and detonation depending on the reaction velocity and the surrounding pressure [1][5].

Combustion is usually approached by reaction kinetic equations which describe the chemical reaction mechanism among the initial components and the newly generated products. In case of burning kerosene, a detailed list of kinetic equations can be found in [6] but to mention only the most important processes in ideal condition, one can find the followings:



Considering the products CO and NO due to incomplete combustion:



Furthermore, to make combustion more realistic, some more phenomena must be taken into account simultaneously as we can see in **Figure 2**.

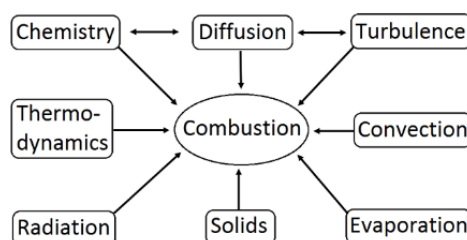


Figure 2 Phenomena related to combustion [7]

The following part of this subchapter provides a deeper insight into the complex fluid dynamic and thermodynamic processes in a combustion chamber. As in 1.1 subchapter turned out, combustor is the heart of gas turbine engines and it has the challenging task of preparing air by raising its power capacity before turbine extracts the energy from the flow of heated gas. Since the air from compressor enters the combustor at around 150 m/s, which is a high velocity for stable flame, the first step is to decelerate it and rise its static pressure in the diffuser. After this, the airflow is split up by the liner. One part of the stream flows through the liner and casing towards the dilution holes, this region is called annulus. The leftover part of the flow enters the mixing chamber. The maximum speed in which kerosene can burn at normal fuel-air ratio is only between 5–10 m/s. If the fuel is in liquid phase, it must be atomized and vaporized with use of special injectors to ensure uniform, homogenous flames and to keep the burning efficiency high. Fuel and air is assumed to be mixed in molecular level and they share same mean velocity, pressure and temperature field. Applying swirler in the mixing chamber, the airflow,

around the fuel nozzle, is further decelerated, the air-fuel mixing is more efficient and a stabilized zone is created, where the enthalpy of hot recirculating gas maintains the flame without using spark ignition again. After mixing, fuel is partially burned in the recirculation zone, but some amount of fuel will not burn completely. The remained fuel quantity will finally burn in the intermediate zone. The hot gases will be then mixed with cooling air in the dilution zone and provide a suitable TIT at the exit of combustor. Dilution holes protect the chamber wall with entering fresh air from severe heat damage, feed and guide the flames towards the outlet.

Considering the mentioned processes above, combustion chamber can be divided into three main sections as shown in **Figure 3**:

- Primary zone (mixing chamber) provides enough time and space for the fuel and air to mix and ignite;
- Secondary zone (intermediate zone) helps to achieve full combustion, thus the level of CO, NO_x and UHC (unburned hydrocarbons) can be reduced;
- Tertiary zone (dilution zone) reduces sufficiently the temperature of hot gases for the turbine blades [1][8].

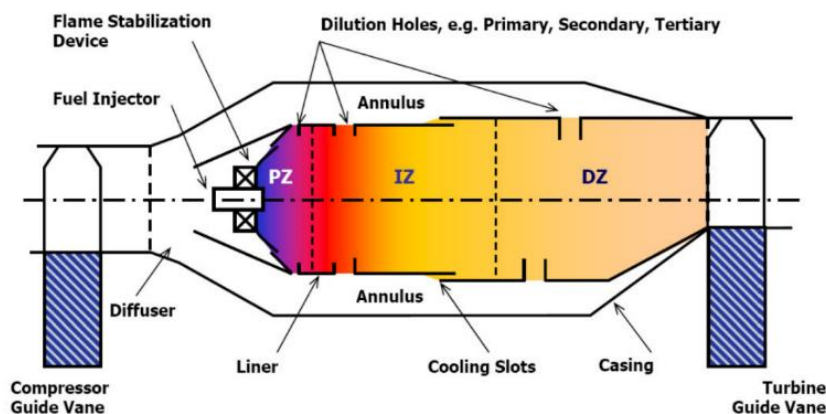


Figure 3 Cross-section scheme of a combustion chamber [8]

After these considerations, we can make the following assumptions as combustion-theory requirements:

- Fuel will ignite only after the injection and evaporation;
- Primary zone is for injection and mixing while the secondary zone is the main region of combustion where the highest proportion of fuel is consumed by the flames;
- Inner wall of combustor is protected against heat damage by cooling air entering through dilution holes along the chamber wall;
- Combustion occurs only in the inner region of combustor and the outer casing remains at ambient temperature;
- Temperature outlet profile is almost uniform and homogenous;
- Temperature of combusted gases leaving the chamber is low enough to avoid the structural disintegrity of turbine blades;

As we can see, combustion is a complex subject which requires the knowledge of many sub-disciplines such as physics, chemistry, fluid dynamics and thermodynamics. Thus engineers have to take into account a wide range of complex phenomena presented in **Figure 2**. Although,

theories and empirical models for turbulent combustion have been created since many decades, the practical use was restricted by the limited computational resources available [9].

1.3 Computational Fluid Dynamics and combustion modelling

From the second part of the 20th century, due to the fast evolution of computer technology and the expectations from the side of industry, the numerical techniques for fluid flow, or in other words Computational Fluid Dynamics (CFD), have become the primary method for solving fluid dynamic problems in engineering sciences. It was originally developed for nuclear and aerospace purpose, but nowadays this the most efficient way of saving cost, capacity and time not only in case of nuclear, aerospace or automotive industry but also in the field of turbo machinery, manufacturing processes, security and building technology, nuclear power, meteorology, environmental protection, astronomy and even in medicine [1][8][10].

CFD solvers are based on the finite volume method in most of the cases which means, the investigated fluid domain is discretized into a set of control volumes (called cells). The general conservation or transport equations for mass (continuity equation), momentum (Navier-Stokes equation), energy, etc. are discretized into a system of algebraic equations which is then solved numerically on this set of control volumes to render the solution field. The need for such and approximated solution is that although the mentioned governing equations, which form a system of nonlinear partial differential equations, have been already known since 150 years, they do not have closed form solution over any kind and size of general and complex flows. Because of this fact, CFD intends to replace the governing equations with numbers, and advance these numbers in space and time in order to obtain a numerical representation of a given flow field but this method usually requires high performance computational technique [10][11].

Turbulence is a chaotic phenomenon in the flow field, when the flow characteristics fluctuate in time and space. This can have a significant effect on the results and can be fully described by the Navier-Stokes equations. Taking into account the turbulence, with statistical averaging and with different turbulence models, the nonlinear partial differential equations can be closed, following the Boussinesq approximation, and numerically solved.

The combustion process can be simulated in CFD, but to describe the fluid accurately, some data such as temperature, pressure, density, velocity and mass flow must be known. Basically, they can be calculated by the governing equations but in case of realistic combustion approach, they have to be completed with reaction kinetic models for the correct flame formation, pollutant models for incomplete combustion, discrete phases models for multiphase flow and particle tracking, heat transfer and radiation models for thermal phenomena and in certain cases with ignition models to initiate the combustion. In terms of reaction kinetic models, combustion depends directly on the mixing process and chemistry. Fast chemistry is limited by the mixing whereas slow reactions are restricted by chemical kinetics. Damköhler-number (D_a) relates the reaction time scale to the convection time scale but it is also defined as the ratio of flow time scale to the chemical time scale [8][10].

If $D_a \gg 1$ chemical reaction is faster than the turbulent mixing but in case $D_a \ll 1$ turbulent mixing plays the main role. In combustion modelling premixed and non-premixed flames can be distinguished regarding when do oxidizer and fuel meet. In case of premixed flame, the

reagents meet each other before the combustion and are used in smaller applications such as internal combustion engines or ovens, however, non-premixed flames occur rather in industrial applications for example in gas turbine engines. [1] Based on the considerations above, CFD offers a huge variety of combustion models and some of them are presented and compared in **Table 1**. PDF Flamelet Model has been used in the present work due to its favourable characteristics for modelling reaction kinetics in gas turbine combustion chamber.

Reaction models	Volume models			Flame models		
	Eddy Dissipation Model	Finite Rate Chemistry Model	Combined EDM-FRCM Model	PDF Flamelet Model	Burning Velocity Model	Extended Coherent Flame Model
Flow	turbulent	laminar or turbulent	turbulent	turbulent	turbulent	turbulent
Reaction speed	fast ($Da \gg 1$)	slow ($Da \ll 1$)	fast and slow	fast ($Da \gg 1$)	fast ($Da \gg 1$)	fast ($Da \gg 1$)
Mixing	non-premixed	premixed	premixed or non-premixed	non-premixed	non-premixed or partially premixed	premixed and partially premixed
Model features	<ul style="list-style-type: none"> • Reaction speed depends on mixing time • Mixing time influenced by vortices • Mixing at molecular level • No kinetic control • Avoid expensive Arrhenius equation calculation 	<ul style="list-style-type: none"> • Reaction speed depends on chemistry • Reaction rates are described by component interactions • Reaction rates are determined by Arrhenius equation calculation 	<ul style="list-style-type: none"> • Mixing time and reaction rates are computed and the smaller is utilized 	<ul style="list-style-type: none"> • Combustion on a thin surface called flamelet • No influence of chemical reaction • Use of probability density function (PDF) • Use of pre-calculated modes 	<ul style="list-style-type: none"> • Flow field is split up burnt and unburnt mixture • Turbulent flame speed correlation • Flame position is determined directly • Turbulent fluctuations • Use of PDF • Use of flamelets 	<ul style="list-style-type: none"> • More sophisticated • Describes extensive and coherent flame, transient combustion process • Transport equation for flame surface • Steady flame
Application	gas phase and coal combustion	gas furnace	liquid combustion	gas turbine combustion chamber	Bunsen burner flame	internal combustion engine

Table 1 Comparison of different combustion models available [7][12][13]

The difficulty of combustion modelling lies in the size. It is called “the computational spatial-scale dilemma” which implies the dynamic range of scales that must be resolved accurately [14]:

- ➔ scale of combustor: 10–100 cm;
- ➔ large eddies in real combustors: 1–10 cm;
- ➔ small-scale mixing occurs at: 0.1–10 mm;
- ➔ droplets with distinct identity: 1–100 μm ;
- ➔ molecular or chemical processes: 0.1–1 nm;

Research and development studies are being released more and more frequently which show the importance and increasing spread of CFD tools in the field of combustion analysis:

In [15] a 2D axisymmetric model of gas turbine combustion chamber was used to investigate the effect of Swirl-number on different multi-objective optimization process such as combustion efficiency, emission, pattern factor and entropy generation minimization. The design criteria of selecting the optimal Swirl-number was discussed in detail and the results were validated with Sydney Swirl Flame Database SM1. According to the results, a region of high swirling flow inside the combustor was identified which is attached to the swirler and characterized with high Swirl-number. Inside this structure there is a region of negative axial velocity and this region is called the internal recirculation zone. High Swirl-number causes high shear zones near the dome walls, hence flame surface is anchored to this region.

In [16] the possibilities of hydrogen fuel, as alternative, renewable and environmentally friendly energy source, was investigated in gas turbine combustion chamber, which does not cause greenhouse gases, ozone layer depleting chemicals, acid rain ingredients or pollution. As it turned out from the results, contrary to the conventional fuel combustion, the high temperature zones are all at the rear of combustion chamber and formation of NO_x happened there, and not near the flames in the middle of the chamber.

In [17] the emission formation using Large Eddy Simulation was successfully reproduced in an industrial gas turbine burner at pressure under laboratory conditions. Large Eddy Simulation turbulence approach allows the analysis of a more detailed turbulent combustion close to the reality. Also the influence of radiation heat losses was investigated and the impact of an alternative four-step chemical mechanism was discussed. The results clearly showed that the thermal radiation has a significant effect on the NO_x formation rates as well as on the flame width and structure.

[18] describes an investigation of “micromix” hydrogen combustion with different combustion models. In this technology, gaseous hydrogen is injected through miniaturized injector nozzles perpendicularly into the air flow. This study helps understanding the flow phenomena related to micromixing, reaction zone, flame and NO_x formation in the combustor. According to the results, miniaturized micro flames developed and anchored at the burner edge of injector nozzle. Reacting time and averaged molar formation of NO_x can be reduced significantly with this type of injection technic. In comparison of different combustion models, Eddy Dissipation Concept showed better agreement against Eddy Dissipation Model or Eddy Dissipation Model – Finite Rate Chemistry model results.

[19] presents a method of experimentally analysed non-stationary thermoacoustic oscillations that can be applied in high-pressure liquid-fuelled gas turbine combustors. The objective of this study was to identify transient regions in which oscillations are being driven or damped based on the dynamics of phase difference between heat release rate and pressure fluctuation. The results allow to study the combustion behaviour inside a liquid-fuelled gas turbine combustor and the temporal evolution of the local phase difference between heat release rate and pressure.

In [20] the focus of the numerical analysis was the fluid dynamics at the combustor – turbine interface and its impact on the turbine blades in case of Cyclone gas turbine. Results were evaluated in

terms of their consistency with temperature indicating point observations obtained during the engine development tests. According to the results, the presence of a highly rotating vortex core was indicated in the combustor. This core is in strong relationship with high temperature peak which is seen to be drawn over the suction surface of the first turbine blades. It is being attracted by the low static pressure in this region but migrates towards the hub through the vane passage.

In [13] a three-dimensional gas phase combustion was modelled in a tubular combustion chamber. The main goal of this investigation was to compare the effect of four different combustion models such as Eddy Dissipation Model, PDF Flamelet model, Burning Velocity Model and Fluent Non-Premixed with real tests. The most accurate results were calculated by Fluent Non-Premixed model and the time-consumption of this combustion model was nearly ten times less than in case of the other models.

2. PROBLEM SOLVING IN CFX

Ansys CFX has been used in the present work to perform coupled fluid dynamic and heat transfer simulations. It is a high-performance fluid dynamics software for general purpose, which has been used for over 20 years to solve a wide range of continuum based engineering problems. The mesh has been generated in the software environment also which provides more opportunities and high level of flexibility for creating appropriate mesh even for a complex geometry such as an annular gas turbine combustion chamber. CFD tools for analysing fluid flow problems can be applied only in case the flow characteristics meet the continuum mechanic requirements. In other words, the Knudsen-number should be smaller than 0.01. In this study the Knudsen-number has been estimated by using the flame temperature and related pressure values (marked by *), based on the results of a very similar CFD analysis [1], in the following way [21][22]:

$$Kn = \frac{\lambda}{L} = \frac{2.005 \cdot 10^{-7}}{0.0001} = \mathbf{0.002} < 0.01 \quad (5)$$

where

mean free path of molecules:

$$\lambda = \frac{R \cdot T}{\sqrt{2} \cdot \pi \cdot d_a^2 \cdot A \cdot p} = \frac{8.3145 \cdot 2090}{\sqrt{2} \cdot \pi \cdot (3.57 \cdot 10^{-10})^2 \cdot 6 \cdot 10^{23} \cdot 254200} = 2.005 \cdot 10^{-7} \text{ m} \quad (6)$$

smallest size of mesh elements: $L = 0.0001 \text{ m}$ gas law constant: $R = 8.3145 \frac{\text{J}}{\text{mol} \cdot \text{K}}$ *flame temperature: $T = 2090 \text{ K}$ *total pressure (related to flame temperature): $p = 254200 \text{ Pa}$ averaged molecule diameter: $d_a = 3.57 \cdot 10^{-10} \text{ m}$ Avogadro's number: $A = 6 \cdot 10^{23} \frac{1}{\text{mol}}$

2.1 Geometry and mesh

The investigated model (see **Figure 4**) is the annular combustion chamber of a modified TSz-21 starting gas turbine for MiG-23 or Szu-22 military aircrafts used in the Hungarian Army. Nowadays it is used for research purpose under the name of TKT-1 gas turbine on the Department of Aeronautics, Naval Architecture and Railway Vehicles at the Budapest University of Technology and Economics. The CAD model of this engine component was available by [1].

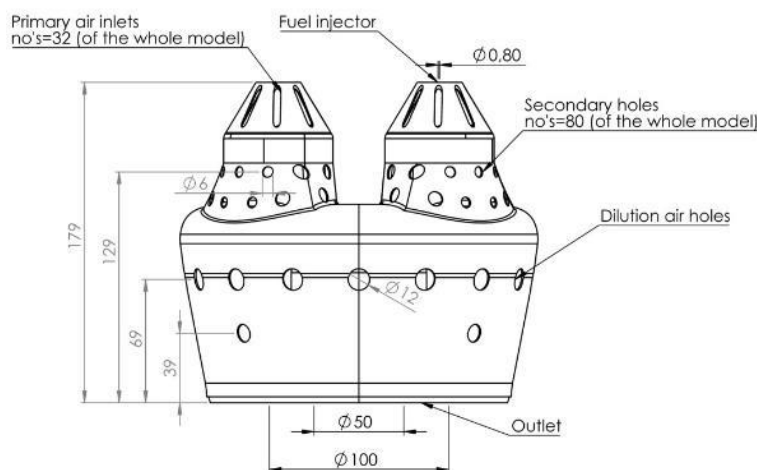


Figure 4 Geometry of investigated combustion chamber [1]

There are several possibilities for selecting the suitable segment of investigated geometry:

- analysis in 2D in the cross-section plane of injector;
- analysis in 3D with a segment angle smaller than 90° ;
- analysis in 3D with segment angle 90° (quarter geometry);
- analysis in 3D with segment angle 180° (half geometry);
- analysis in 3D with segment angle 360° (whole geometry).

It is obvious, that the whole geometry would provide the most realistic results and considering the lower and lower sizes model in the list more and more simplification, inaccuracy and error will be involved in the simulation. Due to time and computational capacity restrictions, only the quarter and half geometry cases have been profoundly investigated in this work.

The numerical mesh must be able to handle the various phenomena related to combustion mentioned in 1.2 subchapter. Tetragonal, non-structured mesh has been generated in order to capture the complexity of the geometry (thin metal sheets close to each other with small holes) and reduce the meshing time. The fuel is injected on a small circular surface so there must be used the smallest mesh elements with maximal edge length of 0.1 mm. There will be generated enough cells (more than 30) for the entering the fluid phase. In primary and secondary zone the mesh must be fine (1 mm) so that the mixing and combustion process can be simulated with high accuracy. Near the solid walls the effect of boundary layer must be taken into account to describe the flow correctly. It demands a short preliminary calculation [21] with volume-averaged temperature (880 K), volume-averaged total pressure (259,784 Pa) and averaged stream velocity (50 m/s) values originated from [1]. The length of combustion chamber is 0.18 m and the target of dimensionless distance of the wall in the first cell is 1. Thus the Reynolds-number:

$$Re = \frac{V \cdot L}{\nu} = \frac{50 \cdot 0.18}{4.33 \cdot 10^{-5}} = 207971.57 \quad (7)$$

the first cell height:

$$y = \frac{y^+ \cdot \nu}{u_\tau} = \frac{1 \cdot 4.33 \cdot 10^{-5}}{2.5} = 1.73 \cdot 10^{-5} \text{ m} = 0.0173 \text{ mm} \quad (8)$$

and the boundary thickness:

$$\delta = 0.035 \cdot L \cdot Re^{-\frac{1}{7}} = 0.035 \cdot 0.18 \cdot 207971.57^{-\frac{1}{7}} = 0.0011 \text{ m} = 1.1 \text{ mm} \quad (9)$$

In case of quarter geometry, the global volume was meshed with 5 mm large mesh elements but at certain parts of the domain, such as primary zone, secondary zone and dilution holes, mesh refinement (1 mm) was applied. An inflation layer was added near the wall with 1.2 mm height (calculated by (9)) and consists of 7 sublayers with 1.5 growth rate. From the simulation results turns out that the real thickness of boundary layer near the wall is corresponding with the calculated value (1.2 mm). The final mesh (see **Figure 5**) was built up from 7,503,619 elements and contains 2,173,562 nodes.

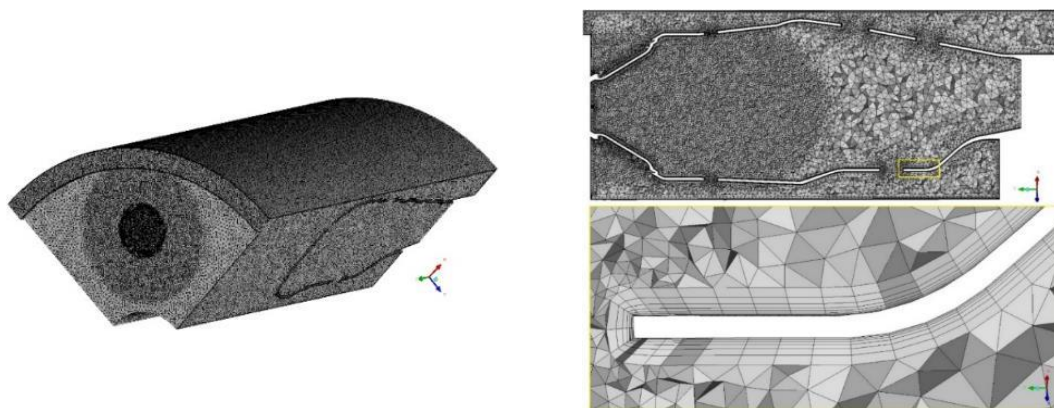


Figure 5 Final mesh of quarter geometry (left) with refinement and inflation layers (right)

The quality of mesh was rated by the worst angle of each mesh element on a scale [0-1], where the accepted angle is considered to be between 30° and 150° . According to the mesh qualification, the mean quality is 0.74 which is acceptable for further investigation. The worst elements are situated in the primary zone, concerning the inlet air holes and swirler sheets. This area is the critical part of the geometry which requires really fine mesh with higher computational capacity. Although mesh sensitivity analyses are going to be completed as a next step of the present work, the used mesh has the best quality that could be reached at this time with considering the available computational resources.

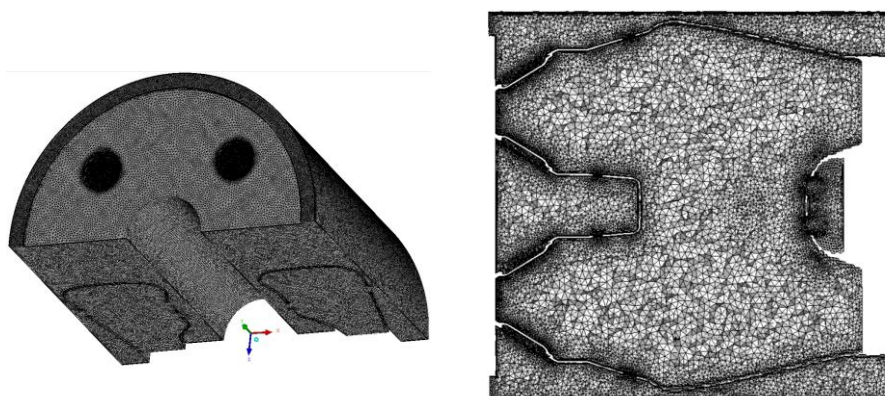


Figure 6 Final mesh of half geometry (left) without refinement (right)

In case of half geometry, the same mesh element-sizes were used with one difference: due to computational capacity limits, mesh refinement could not be applied in the primary and secondary zone and the boundary layer near the walls was split up only for 5 sublayers. Sensibility investigations should be carried out in this case also with higher computational capacity to reveal the

effect of different mesh configuration on the results. The final mesh (see **Figure 6**) was built up from 9,767,342 elements and contains 2,801,512 nodes. The mean quality is 0.7 thus the mesh is in the acceptable range.

2.2 Setting up the simulation

The first step is to define the fuel and the reaction kinetic mechanism. Jet-A (kerosene) was selected for fuel, which can be describe in CFX as a surrogate: 60% n-decane (N C₁₀H₂₂) and 40% trimethylbenzene (TMB C₉H₁₂). An ideal combustion was assumed without NO_x emission. The reaction kinetic equations, which govern the complex kerosene combustion processes and involve every single element and side product, are collected in [6]. The software performs a short calculation (oxidizer-fuel fraction, stoichiometric mixture ratio and composition of combustion product) with use of Flamelet Library and writes the reaction kinetic results in a file.

The second step is to create a gaseous reacting mixture to make burning happen. The file of preliminary calculations, written in the previous step, here can be referred to specify the burning process.

Next step is to couple the liquid and gaseous phases of the fuel by creating a homogenous binary mixture and define the evaporation process with the Antoine-equation coefficients. Evaporation has a significant influence on the combustion since the fraction of each reagents depends on it. In other words, the behaviour of combustion and the flame position is determined by these values. Instead of wasting time to find experimentally the proper coefficients through numerous tests and sensibility simulations, the estimated values have been taken from [23]. With the use of Liquid Evaporation Model, one of the two mass-transport equations will be solved depending on the case if the droplets are above or below the boiling point.

Type of domain	Fluid
Content	Gas mixture and vaporized fuel droplets
Reference pressure	99.75 kPa
Turbulence model	k-ε
Turbulence intensity	5 %
Heat transfer model	Total enthalpy
Combustion model	PDF Flamelet
Thermal radiation model	P 1
Primary break up	Blob method
Secondary break up	Schmehl
Droplet surface tension coefficient	0.026 N/m
Droplet and gas mixture interaction	Fully coupled
Drag force model	Schiller Neumann

Table 2 Applied models and properties of the domain

The Antoine-equation (see equation (10)) determines that the state is above or below the boiling point. Droplets change their phase if the vapour pressure (P_{vapour}) is higher than the ambient pressure:

$$P_{vapour} = P_{scale} \left(A - \frac{B}{T+C} \right) \quad (10)$$

where

- P_{scale} : pressure scale to adjust the pressure unit (1 Pa);
- A : Antoine reference state constant (53.3);

- B : Antoine enthalpy coefficient (5600 K);
- C : Antoine temperature coefficient (25 K);
- T : vaporization temperature.

Afterwards, material properties, reference values, physical settings and boundary conditions are applied on the model (see **Table 2**).

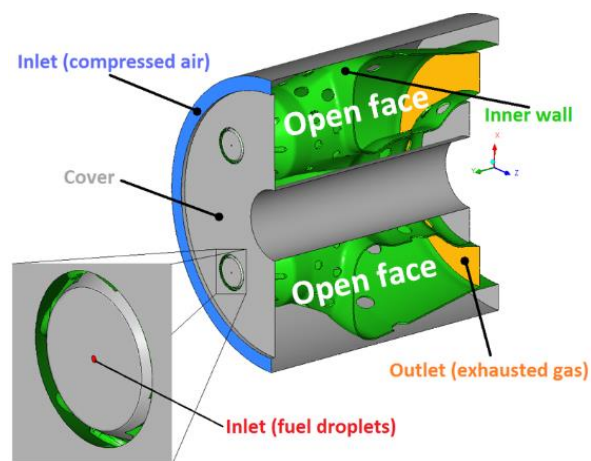


Figure 7 Defined boundary surfaces of the domain

K-epsilon turbulence model is used in this work based on the results of [8]. In this thesis, the effect of different turbulence models, such as k- ϵ , k- ω , SST-k- ω and RSM, were investigated on a 3D, swirling, recirculating combustion process in a can type of experimental combustor. The results were compared to measurement data as well. As it turned out, k- ϵ model is the most acceptable approximation of the combustion process with same boundary conditions. In addition, k- ϵ model provides converged results in less iteration steps than the other models.

Boundary name	Type	Condition
Air inlet	Inlet	Subsonic flow Total pressure: 171723 Pa Flow direction vector: [0.418; -0.82; 0.387] Total temperature: 421.7 K Material: oxidizer
Fuel inlet	Inlet	Subsonic flow Flow direction: Normal to boundary Flow velocity: 12 m/s Mass flow rate: 4.84 g/s Particle diameter: 0.0001 m Static temperature: 299.6 K Material: fuel
Outlet	Outlet	Subsonic flow Mass flow rate: 0.25 kg/s (quarter geometry) Mass flow rate: 0.5 kg/s (half geometry)
Inner wall	Wall	No slip Smooth Adiabatic heat transfer
Cover	Wall	No slip Smooth Heat transfer coefficient: $8 \frac{W}{m^2 \cdot K}$ Outside temperature: 299.6 K
Open faces	Interface	Rotational periodicity around the longitudinal axis (Y)

Table 3 Applied boundary conditions of the domain

The next step was defining the boundary conditions (see **Table 3**) on each boundary surface (see **Figure 7**) based on [1] and [24].

The last step is setting up the solver (see **Table 4**), completing the initialization and running the calculations.

Advection Scheme	High resolution
Turbulence Numerics	First order
Number of iteration	Maximum 1000
Timescale	At beginning: physical (0.01 s); With stabilized results: local (factor 30)
Residual type	RMS
Residual target	10^{-4}
Convergence criteria	1%

Table 4 Applied settings for the solver

Four parameters are created as monitoring points which provide useful information about the fluid flow, thermodynamic processes and convergence during calculation: Maximal temperature (Tmax), Volume-averaged temperature (Tvolume), Area-averaged temperature in the outlet surface (Toutlet) and Area-averaged temperature on the inner wall (Twall).

At combustion analysis, cold flow simulation is a commonly used step before main simulations. In this case, every boundary condition is applied similarly to the main simulation, but combustion and thermal radiation model are switched off. On the one hand, switching on boundary conditions gradually, makes convergence easier and faster. On the other hand, having a closer look at the streamlines without combustion, can reveal any anomaly or discrepancy in the flow field. It can imply incorrect geometries or mesh and even a wrongly defined or missing boundary condition. Because of these reasons, also a cold flow simulation was implemented in this work with quarter geometry before the main calculations.

2.3 Presentation of results

Consistency, stability and convergence play an important role in verification of numerical results. The outcome of a CFD simulation is acceptable for further engineering application if these three properties are proved mathematically. Consistency means that the simplified algebraic equations, which are solved during numerical calculations, capture the content of original nonlinear partial differential equations. Stability proves the fact, that during calculation the numerical result approaches certain values and the difference between each resulted parameters, during the iteration steps, if they are the cases, tends to zero. Convergence ensures that the difference between the exact and numerical solution stays limited during calculation (numerical error does not increase) [11].

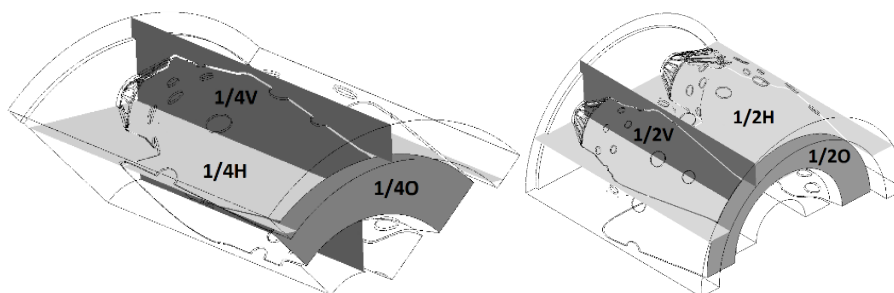


Figure 8 Defined inspections planes for quarter (left) and half geometry (right)

In the following sub-subchapters, the outcome of each CFX simulation will be presented. The results are displayed in 3D view and also with use of perpendicular inspection planes defined in **Figure 8**.

2.3.1 Cold flow results

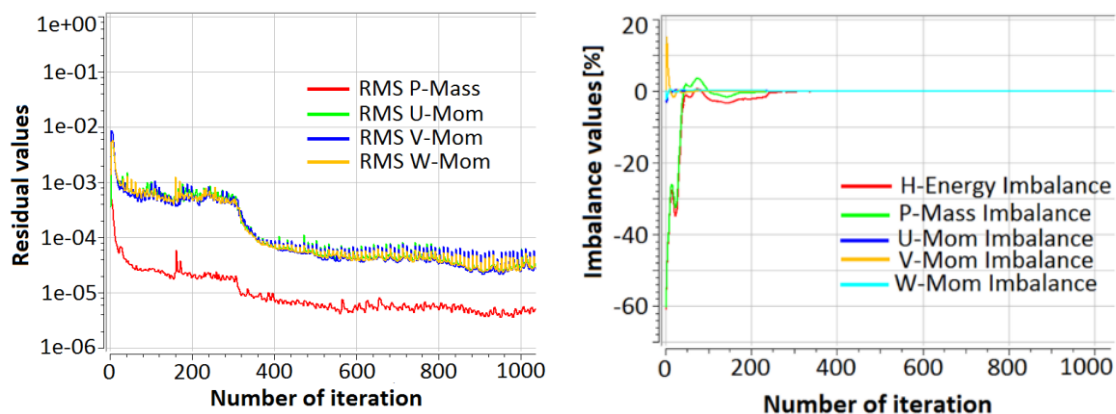


Figure 9 Residual (left) and imbalance curves (right) of cold flow simulation

According to **Figure 9** the imbalance curves ascertain the convergence: each parameter went well below 1% which means the mass, momentum and energy conservation target (after 250 iteration steps) are reached. The residual target of 10^{-4} (after 380 iteration steps) is also reached as well.

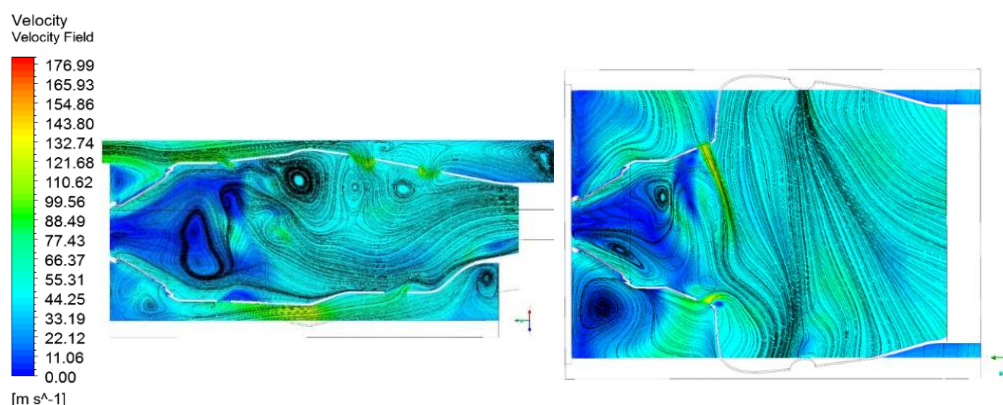


Figure 10 Surface streamlines in 1/4V (left) and in 1/4H (right) planes in case of cold flow

Figure 10 shows the surface streamlines and the velocity field in the background. The prominent feature of this view is the vortex system caused by the complex geometry. The biggest vortices in the primary and secondary zones help the compressed air to slow down (from 100 m/s to 10–20 m/s) and to mix with the vaporized fuel droplets however, the smaller vortices in the corners, between casing and inner wall, are unwanted since they cause pressure loss. There is a temporary velocity increase (130 m/s) around the holes as the air flows through them. It can be clearly seen that the incoming air from compressor is divided correctly into different passages and provides sufficient supply for the chamber in each zone. Due to the lack of combustion and expansion, a dominant flow direction is missing.

2.3.2 Quarter geometry results

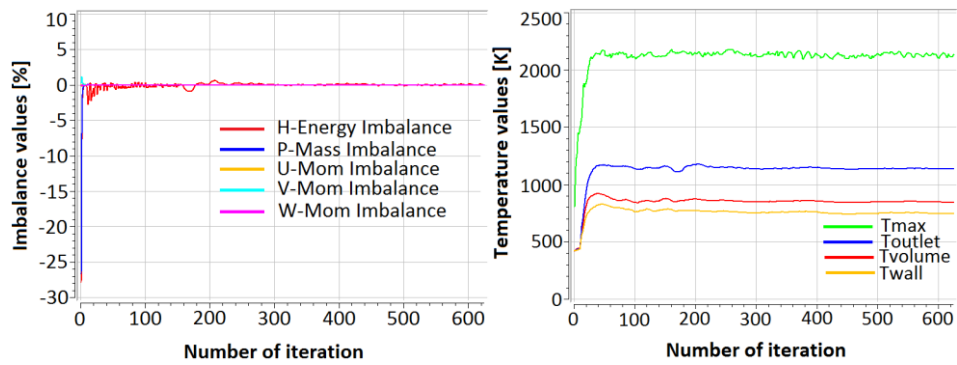


Figure 11 Imbalance (left) and temperature curves (right) of quarter geometry simulation

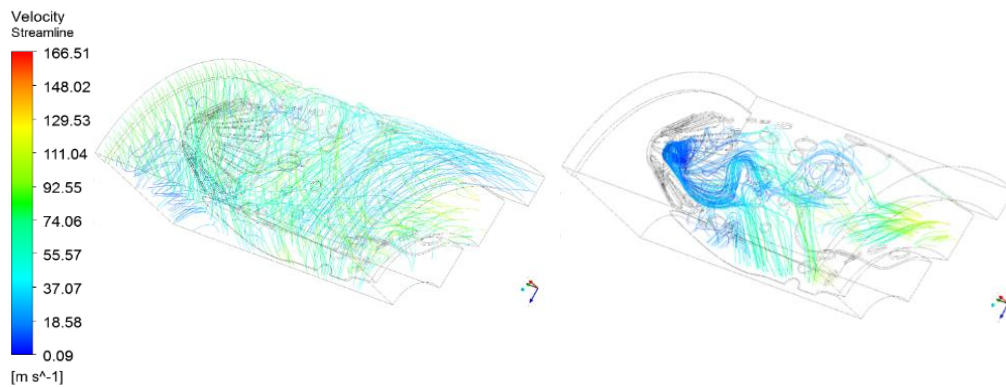


Figure 12 Spatial streamlines of air (left) and fuel (right) of quarter geometry simulation

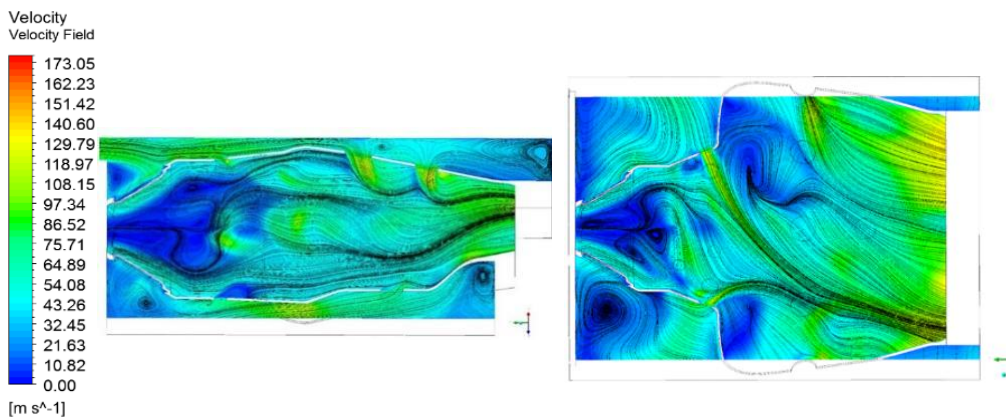


Figure 13 Surface streamlines in 1/4V (left) and in 1/4H (right) planes

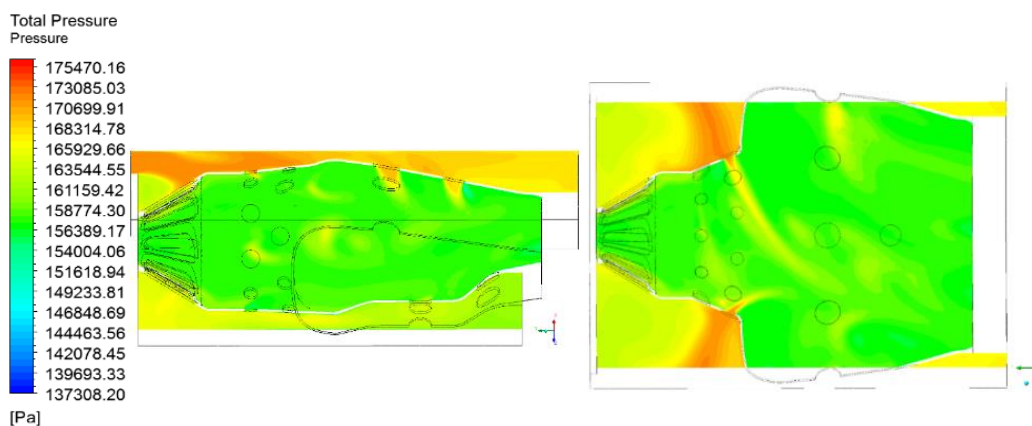


Figure 14 Relative total pressure distribution in 1/4V (left) and in 1/4H (right) planes

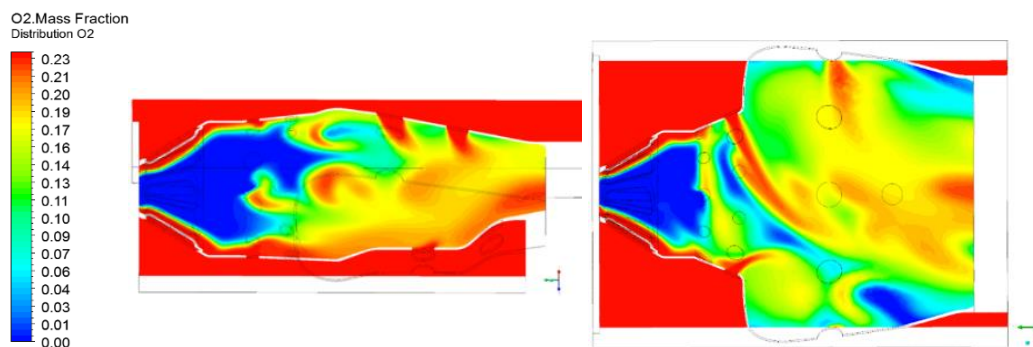


Figure 15 Oxygen distribution (mass fraction in %) in 1/4V (left) and in 1/4H (right) planes

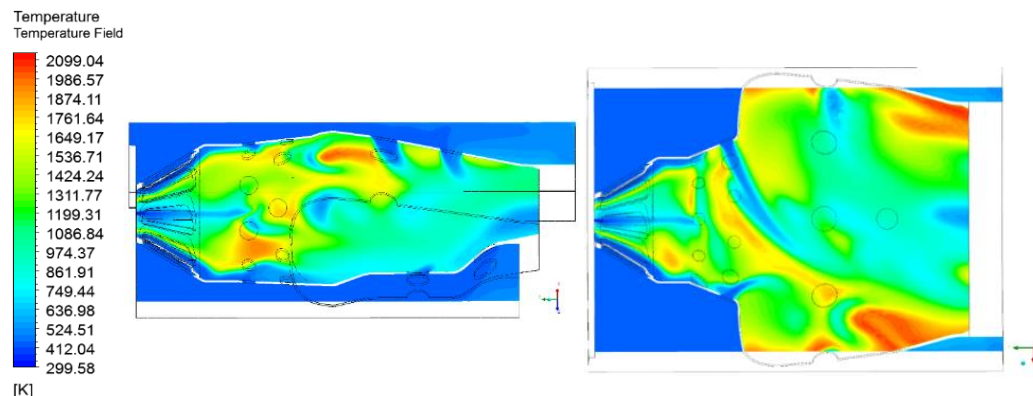


Figure 16 Temperature distribution in 1/4V (left) and in 1/4H (right) planes

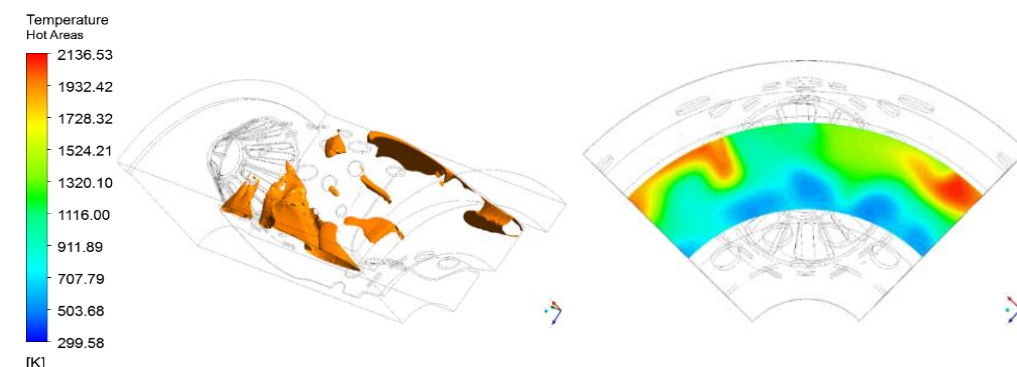


Figure 17 Hot areas (left) and temperature distribution in 1/4O plane (right)

In **Figure 11** the imbalance curves of mass, momentum and energy went below 1%. The area-averaged temperature of inner wall, outlet section and the volume-averaged temperature show clear convergence, the maximal temperature has some minor, continuous fluctuation. In spite of this minor uncertainties, the residual curves converged under the value of 10^{-4} (after 180 iteration steps). The outcome of this simulation is found to be acceptable considering the results as a snapshot of the transient combustion process which is always in change.

Figure 12 shows the spatial streamlines of compressed air and fuel coloured by velocity magnitude in the combustor. The swirler sheets in the primary zone seem to work efficiently as it causes the air slowing down, swirling and helping the vaporized fuel and air to mix each other.

Figure 13 displays surface streamlines and the velocity field in the background. The important bigger vortices and the unwanted smaller vortices can be localized similarly to the cold flow results. The flow shows dominantly axial direction with remarkable velocity increase (around 100 m/s) at the outlet due to the expansion process.

Figure 14 presents the pressure field and gives an explanation for the presented streamlines. As the fluid moves from the higher-pressure inlet to the lower-pressure outlet, it suffers from pressure loss due to collision, friction, separation and swirling. It can be taken into account as $\sigma_{\frac{1}{4}}$ pressure loss factor or $r_{\frac{1}{4}}$ pressure recovery factor which are one of the most important aerodynamical features of a combustion chamber:

$$\sigma_{\frac{1}{4}} = \frac{(\text{surface-averaged total pressure at inlet}) - (\text{surface-averaged total pressure at outlet})}{(\text{surface-averaged dynamic pressure at inlet})} =$$

$$= \frac{271430 \text{ Pa} - 256958 \text{ Pa}}{8493 \text{ Pa}} = 1.704 \quad (11)$$

$$r_{\frac{1}{4}} = \frac{(\text{surface-averaged total pressure at outlet})}{(\text{surface-averaged total pressure at inlet})} = \frac{256958 \text{ Pa}}{271430 \text{ Pa}} = 0.947 \quad (12)$$

Figure 15 reveals the O₂ mass fraction along the flow domain. It confirms the fact that the fuel-air mixing happens sufficiently in the primary and secondary zone and allows to localize the flames where the stoichiometric mixture appears and O₂ mass fraction has a sudden change to zero. Burning occurs on the periphery of blue areas where O₂ is consumed by the flames. The lack of enough amount of cooling air can also be clearly seen in the dilution zone which will cause too high temperature at the outlet.

Figure 16 provides more information about combustion and flame structure in the combustor. The cooling air entering through the dilution holes contributes to the wall protection against heat loads. Even though combustion occurs not only in the secondary zone, the highest temperature flames are anchored to the wall and touching the outlet section as well. Another interesting feature is that the flames return almost to the fuel injection point along the swirler sheets. This implies the fact, that the Antoine-equation coefficients need more refinement in order to delay and describe the combustion process more accurately. The maximal flame temperature of the domain is 2137 K.

Figure 17 shows the flame position near the wall and localizes the high-temperature (2000 K) regions close to the interfaces with rotational periodicity. The temperature distribution in the outlet section is found to be less uniform due to the high temperature peaks. The area-averaged temperature on this surface is 1136.97 K and considering the almost constant tendency of its convergence line, the relative error is 13.7% compared to the expected value of 1000 K used in the preliminary redesign phase. [1]

2.3.3 Half geometry results

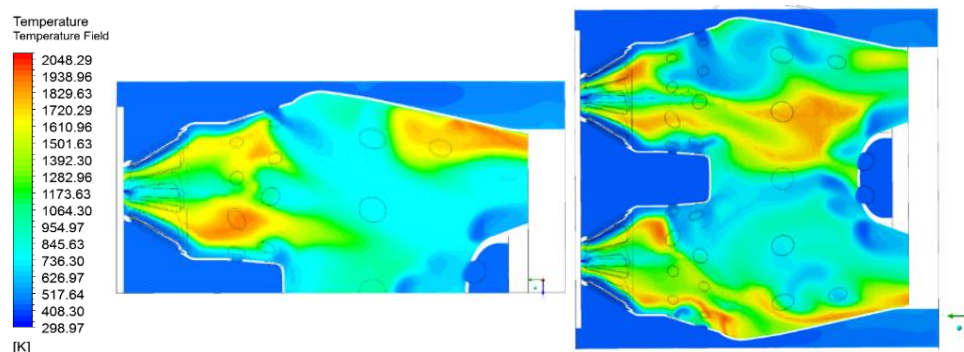


Figure 18 Temperature distribution in 1/2V (left) and in 1/2H (right) planes

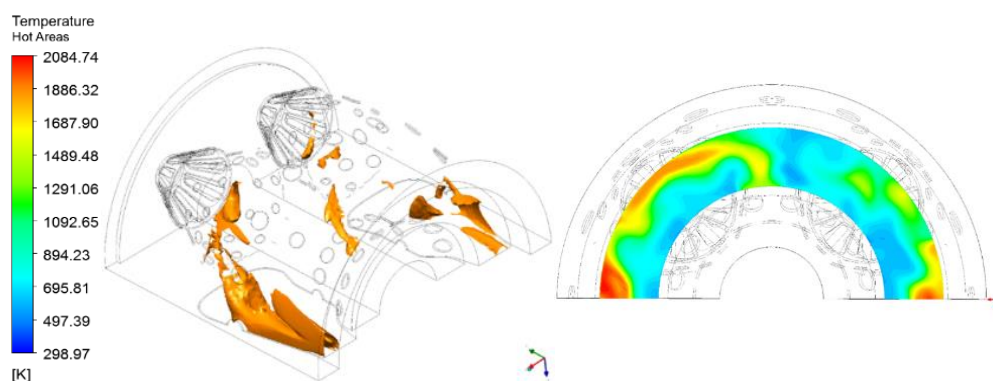


Figure 19 Hot areas (left) and temperature distribution in 1/2O plane (right)

The geometry is doubled, it has rotational periodicity with 180° in the presented simulation case. Spatial streamlines of air and fuel, surface streamlines with velocity field, pressure field and Oxygen mass fraction along the fluid domain show similarities to the quarter geometry results. Bigger amount of cooling air remains in the secondary and dilution zones thus there will be lower temperature peaks at the outlet. The pressure loss factor and recovery factor are:

$$\sigma_{\frac{1}{2}} = \frac{271420 \text{ Pa} - 255470 \text{ Pa}}{8498 \text{ Pa}} = 1.877 \quad (13)$$

$$r_{\frac{1}{2}} = \frac{255470 \text{ Pa}}{271420 \text{ Pa}} = 0.941 \quad (14)$$

Figure 18 displays a more concentrated flame structure which is closer to the ideal combustion features described in 1.2 subchapter. However, combustion develops in the secondary zone, the flames return almost to the injection point thus the combustion process must be fined by the coefficients of Antoine-equation. The maximal flame temperature of the domain is 2085, it is more than 50 K lower than in case of quarter geometry.

Similarly to the quarter geometry results in **Figure 19**, flames are anchored to the wall and the high-temperature (2000 K) regions are situated close to the interfaces of rotational periodicity. The temperature distribution in the outlet section is found to be more uniform due to the lower temperature peaks. The area-averaged temperature in this section is 1037.55 K thus the relative difference is only 3.8% compared to the expected value of 1000 K used in the preliminary redesign phase [1].

2.4 Plausibility check and verification of the results

The goal of the plausibility check and verification is to ensure the correctness of the used method and decide whether the quarter or half geometry simulation provides closer result to a combustion process in a gas turbine engine. Due to the lack of detailed combustion chamber measurement, three different sources have been used to check and verify the presented results.

The video of Yyang CFD Studio [25] gives an insight into a transient combustion process with a very detailed Large Eddy Simulation. All characteristics of an expected combustion (see in 1.2 subchapter) can be found in this video thus it is suitable to check the plausibility of the presented results.

In the both simulations presented in this article, there is a pair of remarkable vortex in the secondary zone that enhances the fuel-air mixing and maintains the flame. The cooling air entering through dilution holes form typical cooler air-sleeves in the hot gases. Additionally, it protects

the wall efficiently against heat damage however, flames tend to anchor to the wall. The combustion occurs only in the inner part of the chamber and flames do not reach the outer regions so casing is not loaded thermally. In case of half geometry simulation, flames have a more concentrated structure similarly to the video. The temperature distribution at the outlet is more uniform with lower temperature peaks and smaller hot-spot areas close to the video results.

As far as concrete temperature and pressure values are concerned, the results of [10] must be considered. In this Master thesis, the quarter geometry of main parts of the original TKT-1 research gas turbine engine was separately investigated with CFD tool and measurements. Methane was used as fuel that shows similar burning characteristics to kerosene.

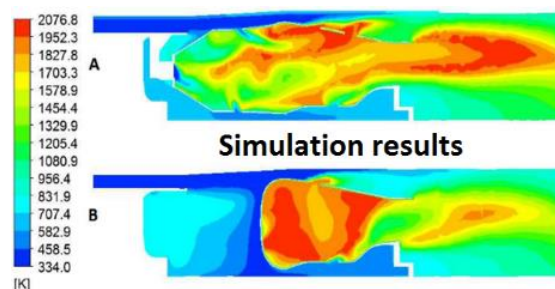


Figure 20 Temperature distribution for verification [10]

Measured and simulated results [10]		
Interfaces	Total Temperature [K]	Total Pressure [Pa]
Ambient-Intake (Measured)	299.6	99755.6
Intake-Compressor (Measured)	299.5	99409.5
Compr.-Combustor (Measured)	414.2	256910
Combustor-Turbine (Simulated)	1008.08	241390
Turbine-Nozzle (Measured)	905.4	114442
Nozzle-Ambient (Measured)	299.6	99755.6

Table 5 Temperatures and pressures for verification [10]

From the view “A” of **Figure 20**, as the cross-section of the combustor, it turns out that flames touch the outlet even in this simulation and causes less uniform temperature distribution in that section. Similarly to the presented results, the high-temperature regions are situated near the interfaces and flames are anchored to the wall, as view “B” the interface section shows. The maximal flame temperature of the domain is 2076.8 K which means only a 2.9% relative difference compared to quarter geometry whereas half geometry results only 0.4% deviation. The area-averaged simulated temperature at the outlet of the combustor is 1008.08 K (see **Table 5**) thus the relative difference is 12.7% with quarter geometry and only 2.9% with half geometry result. According to **Table 5** the pressure loss factor and pressure recovery factor are better than in the present results which can be explained by the modified geometry and slightly different boundary conditions.

$$\sigma_{ver_ [10]} = \frac{256910 \text{ Pa} - 241390 \text{ Pa}}{8100 \text{ Pa}} = 1.92 \quad (15)$$

$$r_{ver_ [10]} = \frac{241390 \text{ Pa}}{256910 \text{ Pa}} = 0.94 \quad (16)$$

In PhD dissertation of [1] the TKT-1 research gas turbine jet engine was redesigned, profoundly CFD analysed, the vanned diffuser is optimized with inverse design method and validated with available measured data. The quarter geometry of combustion chamber is the same that it was

used in this work. Applying similar boundary conditions and fuel, the results are summarized and presented in **Figure 21** and **Figure 22**.

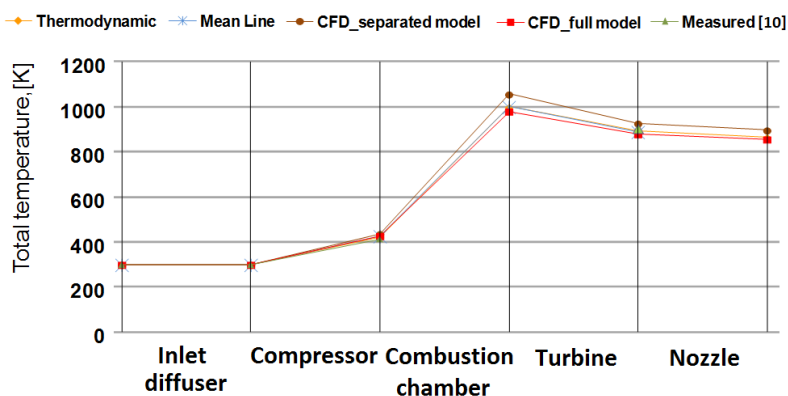


Figure 21 Total temperatures along the TKT-1 research jet engine by [1] for verification

The maximal flame temperature of the domain is 2247 K, thus the relative difference is 4.9% with quarter geometry result, whereas the case of half geometry causes 7.2% deviation. The area-averaged temperature at the outlet is 1056 K which means 7.7% relative difference compared to the quarter geometry simulation but in case of half geometry this difference is 1.8 %.

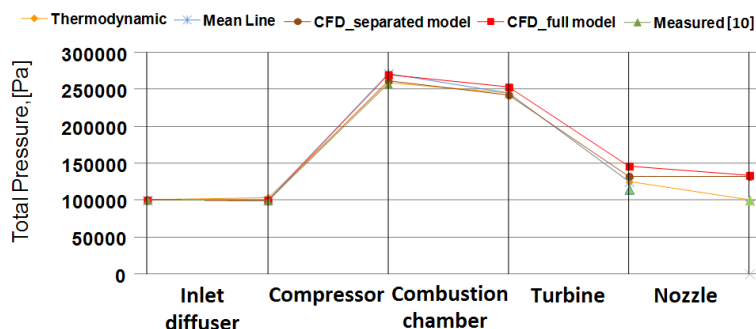


Figure 22 Total pressures along the TKT-1 research jet engine by [1] for verification

Pressure loss factor and pressure recovery factor show similarities with the presented results:

$$\sigma_{ver_ [1]} = \frac{271750 \text{ Pa} - 254750 \text{ Pa}}{8694 \text{ Pa}} = 1.955 \quad (17)$$

$$r_{ver_ [1]} = \frac{254750 \text{ Pa}}{271750 \text{ Pa}} = 0.94 \quad (18)$$

Based on the results discussed above, it can be concluded that the presently simulated results are plausible, they are verified by three different approaches. As far as relative differences of the outlet area-averaged temperature of combustion chamber are concerned, the average differences are below 11 %. In case of quarter geometry, this value is

$$\frac{12.7 + 7.7}{2} = 10.2\% \quad (19)$$

whereas for half geometry it is

$$\frac{2.9 + 1.8}{2} = 2.4\% \quad (20)$$

Hence, since the later one shows better agreement with the outcomes of the mentioned investigations, it is proposed for future use. However, mesh size and configuration with model and

solver parameter sensitivity analyses should be completed beside measurement based validation as next step of this investigation to recover better the limitations of the present method.

3. CONCLUSION

Coupled fluid dynamic and heat transfer simulations were completed on an annular combustion chamber of a TKT-1 small-sized research gas turbine engine with CFD tool. The main goal of this study is to analyse the combustion process and to find the suitable geometrical configuration which describes accurately and in realistic way the phenomena in gas turbine combustion chamber. Quarter and half segments of the chamber geometry was investigated with same boundary conditions. Considering the summarized results in **Table 6**, the quarter and also the half geometry calculations provided acceptable results as well. However, the outcome of half geometry simulation is found to be more realistic approximation of combustion process regarding verification data and preliminary redesign values. Nonetheless, the weaknesses of the applied mesh, interface boundary condition and evaporation model were also highlighted. The need for mesh refinement and sensibility studies with higher computational capacities were emphasized. It also turned out that not only the properly selected boundary conditions but also the size of the investigated geometry segment has significant influence on the turbine inlet temperature. Hence, further investigations and measurements are desirable to improve the actual results.

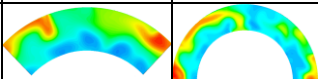
	Quarter geometry	Half geometry	Relative differences for verification by [10] (see Table 5)		Relative differences for verification by CFD results of [1]	
			Quarter	Half	Quarter	Half
Pressure loss factor	1.704	1.877	11.3 %	2.2 %	12.8 %	4 %
Pressure recovery factor	0.947	0.941	0.8 %	0.1 %	0.8 %	0,1 %
Maximal flame temperature	2137 K	2085 K	2.9 %	0.4 %	4.9 %	7.2 %
Outlet area-averaged temperature	1136.97 K	1037.55 K	12.7 %	2.9 %	7.7 %	1.8 %
Relative difference to 1000 K	13.7 %	3.8 %				
Number of mesh elements	7503619	9767342				
Temperature distribution at outlet						

Table 6 Summary of the results with the relative differences

ACKNOWLEDGEMENTS

The present research is partially supported by the Hungarian national EFOP-3.6.1-16-2016-00014 project. The introduced and verified calculation method is carried out to be applied in small aircraft hybrid propulsion system development supported by Hungarian national EFOP-3.6.1-16-2016-00014 project entitled by “Investigation and development of the disruptive technologies for e-mobility and their integration into the engineering education”.

BIBLIOGRAPHY

- [1] Foroozan Zare, Dr. Veress Árpád: Advanced Research on Gas Turbine Components – Virtual Prototyping of Jet Engines, PhD dissertation, Budapest University of Technology and Economics, Budapest, 2017
- [2] Vinod Srinivasa: CFD for Aero Engines, HCL Technologies, 2011, (online), url: https://www.hcltech.com/sites/default/files/resources/whitepaper/files/2011/07/19/CFD_for_Aero_Engines.pdf (04.03.2017.)
- [3] P. Meherwan: Gas turbine engineering handbook, Elsevier’s Science&Technology Rights, Texas,USA, 2011

- [4] YXLON: Inspecting turbine blades non-destructively, (online), url: <http://www.yxlon.de/Applications/Cast-parts/Turbine-blades> (04.03.2017.)
- [5] Md Abdul Alim: CFD Modelling of Turbulent Combustion and Heat Transfer, Loughborough University Institutional Repository, Loughborough, 2004, (online), url: <https://dspace.lboro.ac.uk/dspace-jspui/bitstream/2134/7639/2/Thesis-2004-Alim.pdf> (04.03.2017.)
- [6] S. Honnet, K. Seshadri, U. Niemann, N. Peters: A Surrogate Fuel for Kerosene, Mc Gill University, Montreal, 2008, (online), url: https://www.itv.rwth-aachen.de/fileadmin/Downloadbereich/Comb_Symp08_Kerosene_Honnet_et_al_App.pdf (04.03.2017.)
- [7] Carlos Eduardo Fontes, Raphael David A. Bacchi: Best Practice Guidelines for Combustion Modelling, Ansys South American Conference & ESSS Users Meeting, Atibaia, 2010, (online), url: http://www.esss.com.br/events/ansys2010/pdf/20_2_1630.pdf (04.03.2017.)
- [8] Tajti József, Bicsák György: The Influence of Different Turbulence Models on Gas Turbine Combustion Process with Particular Regard to the Temperature Distribution, BSc. Thesis, Budapest University of Technology and Economics, Budapest, 2015
- [9] Ali Hussain Kadar: Modelling Turbulent Non-Premixed Combustion in Industrial Furnaces, MSc. Thesis, Delft University of Technology, Delft, 2015, (online), url: http://ta.twi.tudelft.nl/users/vuik/numanal/kadar_afst.pdf (04.03.2017.)
- [10] Pallag Nándor, Beneda Károly: A TKT-1 gázturbinás sugárhajtómű áramlástanai vizsgálata, diplomaterv, Budapesti Műszaki és Gazdaságtudományi Egyetem, Budapest, 2013
- [11] Dr. Veress Árpád: Bevezetés az áramlástan numerikus módszereibe, Budapesti Műszaki és Gazdaságtudományi Egyetem, tanszéki oktatási segédlet, Budapest, 2002, (online), url: http://www.vrht.bme.hu/letoltes/Tanszeki_letoltheto_anyagok/Oktatok_anyagai/Dr.Veress_Arpad_anyagai/Oktatot_targyak/Bevezetes_a_numerikus_aramlastanba_CFD/CFD-jegyzet.pdf (04.03.2017.)
- [12] Dr. Veress Árpád: CFD számítási sablon, Budapest University of Technology and Economics, Budapest, 2014, (online), url: <http://www.vrht.bme.hu/hu/hallgatoinknak/letoltesek.html> (04.03.2017.)
- [13] György Bicsák, Anita Hornyák, Dr. Árpád Veress: Numerical Simulation of Combustion Processes in Gas Turbine, Budapest University of Technology and Economics, Budapest, 2012, (online), url: <http://tehetseg.bme.hu/?letoltes/ecc166f70b53c784c4f4dbfb27f8ba029b6fbb8c/a438906f8e3a0fb2b29835505ef39c41c4cb036f/1423/47b0b717d84c1f0c70c264262153ad18f9e3430f> (04.03.2017.)
- [14] Heinz Pitsch, Suresh Menon: CFD for Combustion Modeling, Lecture PPT, Georgia Institute of Technology, Atlanta, 2015, (online), url: <http://www.ccl.gatech.edu/sites/default/files/CCL/Papers/2011/Reports/CFD11-Day2-Lecture1.pdf> (04.03.2017.)
- [15] M.M. Torkzadeh, F. Bolourchifard, E. Amani: An Investigation of Air-Swirl Design Criteria for Gas Turbine Combustors Through a Multi-Objective CFD Optimization, Amirkabir University of Technology, Teheran, 2016, (online), url: <http://www.sciencedirect.com/science/article/pii/S0016236116308791> (04.03.2017.)
- [16] Jianzhong Li, Li Yuan, Hukam C. Mongia: Simulation of Combustion Characteristics in a Hydrogen Fuelled Lean Single-Element Direct Injection Combustor, Elsevier Ltd, 2016, (online), url: <http://www.sciencedirect.com/science/article/pii/S0360319916332517> (04.03.2017.)
- [17] G. Bulat, W.P. Jones, A.J. Marquis: NO and CO Formation in an Industrial Gas-Turbine Combustion Chamber Using LES with the Eulerian Sub-Grid PDF Method, Elsevier Ltd, 2014, (online), url: <http://www.sciencedirect.com/science/article/pii/S0010218014000042> (04.03.2017.)
- [18] A. Haj Ayed, K. Kuserer, H.H.-W. Funke, J. Keinz, C. Striegan, D. Bohn: Experimental and Numerical Investigations of the Dry-Low-NOx Hydrogen Micromix Combustion Chamber of an Industrial Gas Turbine, Elsevier Ltd, 2015, (online), url: <http://www.sciencedirect.com/science/article/pii/S2212540X15000504> (04.03.2017.)
- [19] S. Kheirkhah, B.D. Geraedts, P. Saini, K. Venkatesan, A.M. Steinberg: Non-Stationary Local Thermoacoustic Phase Relationships in a Gas Turbine Combustor, Elsevier Ltd, 2016, (online), url: <http://www.sciencedirect.com/science/article/pii/S1540748916304217> (04.03.2017.)
- [20] Mark D. Turrell, Philip J. Stopford, Khawar J. Syed, Eoghan Buchanan: CFD Simulation of the Flow Within and Downstream of a High-Swirl Lean Premixed Gas Turbine Combustor, Proceedings of ASME Turbo Expo 2004 Power for Land, Sea and Air, Vienna, 2004, (online), url: <https://pdfs.semanticscholar.org/10dd/16fe068c64189894e2e79ae2399ec29b5916.pdf> (04.03.2017.)
- [21] Dr. Veress Árpád: Hő-és áramlástanai számítások, Előadásjegyzet, Budapesti Műszaki és Gazdaságtudományi Egyetem, Budapest, 2016, (online), url: http://www.vrht.bme.hu/letoltes/Tanszeki_letoltheto_anyagok/Oktatok_anyagai/Dr.Veress_Arpad_anyagai/Oktatot_targyak/Ho-es_aramlastani_szamitasok/CFD_v1.pdf (04.03.2017.)

- [22] Widener University: Mean Free Path vs Pressure Altitude, (online), url: <http://science.widener.edu/~svanbram/chem332/pdf/menfpath.pdf> (04.03.2017.)
- [23] Matej Zadavec, Bostjan Rajh, Niko Samec, Matjaz Hribersek: Numerical Analysis of Oil Combustion in a Small Combustion Device, University of Maribor, Maribor, 2014, (online), url: http://www.analipazu.si/sites/default/files/Separat_Numerical_analysis_of_oil_combustion.._0.pdf (04.03.2017.)
- [24] G. Manoj Kumar, J. Bruce Ralphin Rose: Numerical Comparative Study on Convective Heat Transfer Coefficient in a Combustor Liner of Gas Turbine with Coating, International Journal of Mechanical Engineering and Research, Tamil Nadu, 2015, (online), url: https://www.ripublication.com/ijmer_spl/ijmaerv5n1spl_03.pdf (04.03.2017.)
- [25] YYang CFD Studio: Gas Turbine Combustor LES Simulations, video, (online), url: <https://www.youtube.com/watch?v=Mim33CvQTUQ> (04.03.2017.)

KISMÉRÉTI KÍSÉRLETI GÁZTURBINÁS SUGÁRHAJTÓMŰ ÉGÉSTERÉBEN LEJÁTSZÓDÓ FOLYAMATOK CSATOLT ÁRAMLÁSTANI ÉS TERMIKUS VIZSGÁLATA

Gázturbinás sugárhajtóművek tervezési és fejlesztési fázisában elengedhetetlen a hajtómű főbb részeiben lejátszódó összetett fizikai, kémiai, áramlástani és termikus jelenségek ismerete. Numerikus eszközök és vizualizációs technikák alkalmazásával a mérnökök képesek feltárni és jobban megérteni a gázturbinás sugárhajtóművek belső zajló összetett és rejtett folyamatokat. Ezen tanulmány célja egy kisméretű kísérleti gázturbina égésterében lezajló csatolt áramlástani és termikus folyamatok szimulációja és vizsgálata numerikus eszközökkel különös tekintettel az égési folyamat helyességére és a kilépési hőmérséklet eloszlására összevetve égéseméleti követelményekkel és a rendelkezésre álló, verifikációra alkalmas adatokkal. A plauzibilitás ellenőrzésére egy korábbi MSc diplomaterv és egy folyamatban lévő doktori disszertáció eredményei felhasználásra kerültek azonos geometria és hasonló vizsgálati körülmények és célok mellett.

Kulcsszavak: *égéster, égésmodellezés, gázturbinás sugárhajtómű, numerikus áramlástan, turbina belépő hőmérséklet*

Venczel Márk (BSc) MSc. hallgató Budapesti Műszaki és Gazdaságtudományi Egyetem venczelmark@freemail.hu orcid.org/0000-0002-4319-1463	Venczel Márk (BSc) MSc. Student Budapest University of Technology and Economics venczelmark@freemail.hu orcid.org/0000-0002-4319-1463
Bicsák György (MSc) tanársegéd Budapesti Műszaki és Gazdaságtudományi Egyetem Vasúti Járművek Repülőgépek és Hajók Tanszék gybicsak@vrht.bme.hu orcid.org/0000-0002-3427-3918	Bicsák György (MSc) Assistant lecturer Budapest University of Technology and Economics Department of Aeronautics Naval Architecture and Railway Vehicles gybicsak@vrht.bme.hu orcid.org/0000-0002-3427-3918
Dr. Veress Árpád (PhD) docens Budapesti Műszaki és Gazdaságtudományi Egyetem Vasúti Járművek Repülőgépek és Hajók Tanszék averess@vrht.bme.hu orcid.org/0000-0002-1983-2494	Dr. Veress Árpád (PhD) Associate professor Budapest University of Technology and Economics Department of Aeronautics Naval Architecture and Railway Vehicles averess@vrht.bme.hu orcid.org/0000-0002-1983-2494



http://www.repulestudomany.hu/folyoirat/2017_2/2017-2-14-0391_Venczel_M-Bicsak_Gy-Veress_A.pdf

